PMU Assisted Integrated Impedance Angle Based Microgrid Protection Scheme

Presenter: Nikhil Kumar Sharma, Research Scholar, School of Electrical Sciences, IIT, Bhubaneswar
Supervisor: Dr. S. R. Samantaray, Associate Professor, School of Electrical Sciences, IIT, Bhubaneswar

National Science Day 10th Research Scholars' Day 2020 IIT Bhubaneswar

INTRODUCTION

Microgrid

The microgrid, can be defined as "a group of interconnected loads and distributed energy resources (DERs) with clearly defined electrical boundaries that acts as a single controllable entity with respect to the grid and can connect and disconnect from the grid to enable it to operate in both grid-connected or island modes"

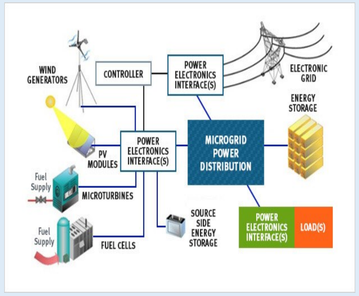

Fig. 1. Microgrid Architecture

Challenges in Microgrid Protection

- Bi-directional Flow of Power
- Variation in Fault Levels
- Blinding of Protection System
- Loss of Relay Coordination
- Auto Re-closure Failure
- Unintentional islanding

Performance of Overcurrent and Differential Scheme for Microgrid

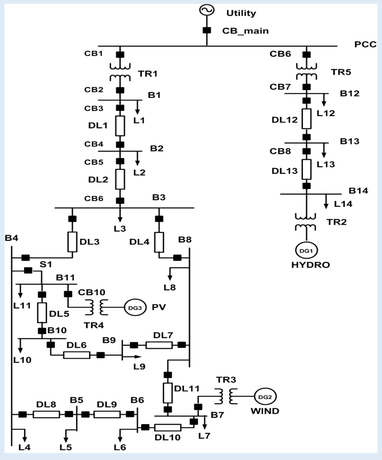

Fig. 2. Microgrid testbed [1]

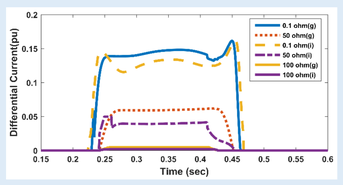

Fig. 3. Responses of differential relay for LG fault at the midpoint of DL9

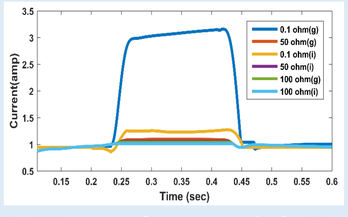

Fig. 4. Responses of overcurrent relay for LG fault at the midpoint of DL9

MOTIVATION

- Development of a relaying scheme which can protect the microgrid with wide variation in operating conditions and fault scenarios
- Inclusion of wide area monitoring system for time-stamped, accurate and faithful measurement
- The scheme should be insensitive for external faults, short transients and switching

PROPOSED SCHEME

Integrated Impedance Angle (IIA) Based Protection Scheme

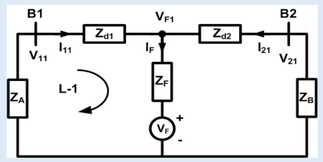

Fig. 5. Pure fault component network with an internal fault

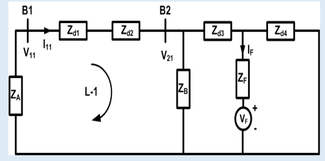

Fig. 6. Pure fault component network with an external fault

The integrated impedance angle [2] is defined as:

$$IIA = \arg\left(\frac{V_{11}+V_{21}}{I_{11}+I_{21}}\right)$$

(a) For internal faults:

$$IIA = \arg\left[-\frac{1}{2}\left(Z_A + \frac{Z_1 Z_B}{Z_2}\right)\right]$$

(b) For internal faults without DG:

$$IIA = \arg\left[-\frac{1}{2}\left(Z_A + \frac{Z_1}{Z_{d2}}\right)\right]$$

(c) For external faults:

$$IIA = \arg\left(Z_B + \frac{Z_d}{2}\right)$$

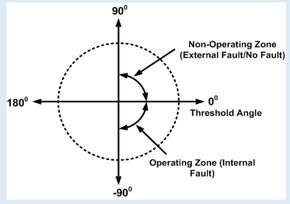

Fig. 7. Operating characteristics of the proposed scheme

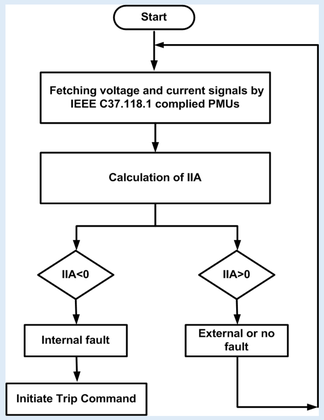

Fig. 8. Flowchart of the proposed scheme

RESULTS AND DISCUSSIONS

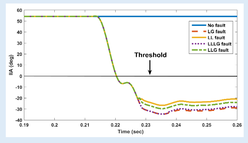

(a)

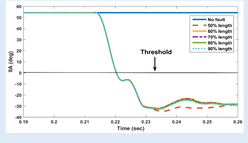

(a)

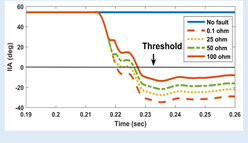

(a)

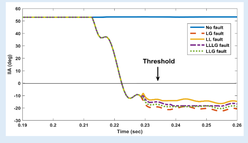

(b)

Fig. 9. Variation in IIA with different fault types at the midpoint of the line DL9 with RF=0.1 Ω in (a) grid-connected mode (b) islanding mode

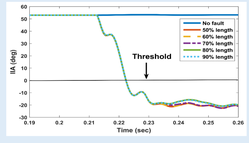

(b)

Fig. 10. Variation in IIA with fault location at the line DL9 for LG fault with RF=0.1 Ω in (a) grid-connected mode (b) islanding mode

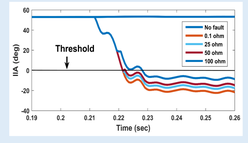

(b)

Fig. 11. Variation in IIA with fault resistance at the midpoint of the line DL9 for LG fault in (a) grid-connected mode (b) islanding mode

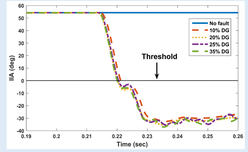

Fig. 12. Variation in IIA with variation in DG penetration at the midpoint of DL9 in grid-connected mode for LG fault with RF =0.1 Ω.

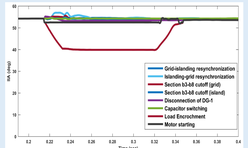

Fig. 13. Performance of the relay for no fault critical cases

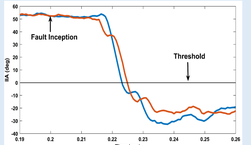

Fig. 14. Impact of measurement noise on IIA monitored by relay placed at bus B5 for LLLG fault at the midpoint of line DL9

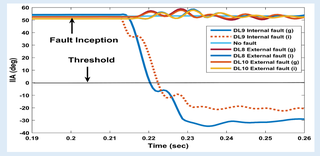

Fig. 15. Performance of the relay for external LG fault at the mid-point of line DL8 and DL10 with RF =0.1 Ω

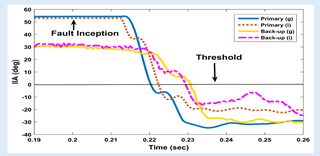

Fig. 16. Performance of the relay at bus B4 as backup relay for LLLG fault at the mid-point of line DL9 with RF =0.1 Ω

Validation on IEEE 34 Bus Microgrid

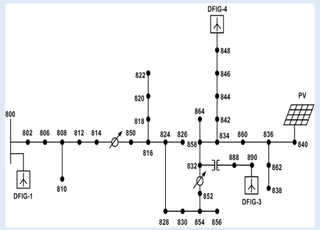

Fig. 17. IEEE 34 bus test node

The proposed scheme is validated on an IEEE 34 bus test system integrated with the distributed generation. The test system is integrated with 3 wind turbines, each of rating 660 kW and one solar farm of rating 250 kW placed at different nodes of the distribution system.

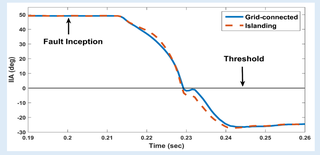

Fig. 18. IIA during LG fault at midpoint of node 816 and 824 with RF = 0.1 Ω

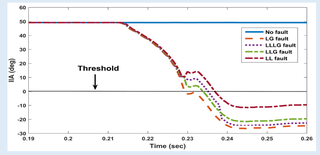

Fig. 19. Variation in IIA with different fault types at the midpoint of node 816 and 824 in the grid-connected mode with RF =0.1 Ω

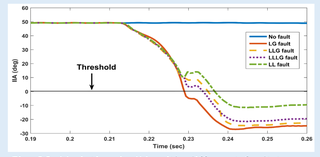

Fig. 20. Variation in IIA with different fault types at the midpoint of node 816 and 824 in the islanding mode with RF =0.1 Ω

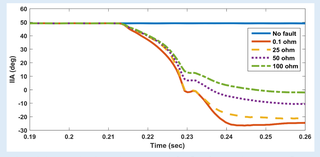

Fig. 21. Variation in IIA with fault resistance for LG fault occurring at the midpoint of node 816 and 824 in the grid-connected mode

CONCLUSION

- The proposed IIA based scheme is capable of detecting the fault for different fault types, fault locations and fault resistances for grid-connected as well as islanding mode of operation.
- The proposed scheme remains stable during the critical no fault issues and is also capable of providing backup protection to the adjacent line with appropriate time delay.
- The proposed scheme can be a potential candidate for developing centralized protection schemes using emerging low-cost micro-PMUs and high-speed communication technology for the future smart microgrid.

REFERENCES

1. S. R. Samantaray, I. Kamwa and G. Joos, "Phasor measurement unit based wide-area monitoring and information sharing between micro-grids," in IET Gen. Trans. & Dist., vol. 11, no. 5, pp. 1293-1302, March- 2017.
2. J. Suonan, K. Liu and G. Song, "A Novel UHV/EHV Transmission-Line Pilot Protection Based on Fault Component Integrated Impedance," in IEEE Transactions on Power Delivery, vol. 26, no. 1, pp. 127-134, Jan. 2011.
3. I. Kamwa, S. Samantaray, and G. Joos, "Compliance analysis of PMU algorithms and devices for wide-area stabilizing control of large power systems," in IEEE Trans. Power Syst., vol. 28, no. 2, pp. 1766–1778, May 2013.